Journal of Applied Mechanics Vol. 1 (August 1998) JSCE

Failure Simulation of Foundation by Manifold Method And Comparison with Experiment

マニフォールド法による基礎破壊のシミュレーションと実験結果の比較

Guoxin Zhang*, Yasuhito Sugiura and Kozo Saito*****
張 国新・杉浦 靖人・斎藤 孝三
*INA Corporation. (1-44-10 Sekiguchi Bunkyoku, Tokyo)
**INA Corporation. (1-44-10 Sekiguchi Bunkyoku, Tokyo)
***Member, INA Corporation. (1-44-10 Sekiguchi Bunkyoku, Tokyo)

Manifold Method (MM) is a newly developed numerical tool in analyzing both continuous and discontinuous problems. By employing the concept of cover and two sets of meshes, MM can simulate the small and large-scale deformation of materials as well as the failure and movement of block system. In the present paper the original MM is extended by adding the consideration of crack propagation in failure process into the numerical procedure. The extended version of MM is then applied to simulate the initiation and propagation of cracks in dam foundation with weak zone such as faults and joints. The failure process and corresponding bearing capacity are predicted, and the computed results are compared with those of the experiment. It is convinced that the extended version of MM can reproduce the initiation of cracks and the failure process reasonably well.

Key Words: Manifold Method, blocks, discontinuity, failure

1. Introduction

Several numerical methods are used in simulating the failure and response of structure and rock foundation with discontinuities. These methods include the Finite Element Method (FEM), the Boundary Element Method (BEM), the Discrete Element Method (DEM) and the Discontinuous Displacement Analysis (DDA). Although discontinuities in structure and rock mass can be modeled in a discrete manner with FEM and BEM by using special joint elements (such as Goodman Element), it is difficult to describe the discontinuities numerically, and small deformation restriction is usually needed. And also the number of discontinuities that can be handled is limited. Therefore, problems of many discontinuities or large-scale deformation can not be analyzed by such kind of methods. DEM and DDA can be utilized to model the behavior of structure with many discontinuities or block system, but the stress distribution inside the blocks can not be calculated properly, and, therefore, the propagation of cracks through blocks can not be well modeled.

Manifold Method (MM) proposed by Shi in 1991[1] is a new numerical method. It provides a unified framework for solving problems with both continuous and discontinuous media. The concept and potential application of this method have drawn a great attention from international researchers in engineering fields[2) 3) 4) 5) 6) 7) 8)].

By employing the concept of cover and two sets of meshes, manifold Method combined the advantages of FEM and DDA. It can not only deal with discontinuities, contact, large scale deformation and block movement as DDA, but also provide the stress distribution inside each block accurately as FEM can.

In the present paper, the original Manifold Method is extended to simulate the failure of existing joints and the propagation of cracks

inside blocks. As examples, the failure of two dam foundations is simulated by the extended MM and the results are compared with those of the experiment.

2. Basic Concepts of Manifold Method

2.1 Cover and Two Sets of Meshes

The most innovative features of Manifold Method are the concept of cover and the use of two sets of meshes. Every cover covers a fixed area, the shape and size of this area can be chosen freely according to the problem to be solved. The covers overlap each other and cover the whole physical area. In each cover, a local function is defined. By means of weight function, the local functions are combined to form the global function and define the displacement and stress in the whole region.

The two sets of meshes are physical meshes and mathematical meshes. The physical meshes describe the physical domain including boundaries, joints and the interfaces between blocks, and define the integration area. The physical meshes are definitely determined by the problem to be analyzed. The mathematical meshes, on the other hand, are closed lines selected more or less arbitrarily by users. The enclosed areas by the mathematical meshes are called mathematical covers, on which the space function is built. The mathematical meshes should be large enough to cover every point of the physical meshes.

The physical and mathematical meshes intersect each other and form the physical covers. If the physical meshes divide a mathematical cover into two or more completely disconnected domains, these domains are called as physical covers.

All the closed areas generated by the intersection between physical meshes and mathematical meshes are defined as the calculation elements. One calculation element may be covered by one or more physical covers, and its behavior is determined by these covers.

Fig.1 gives an example of general covers of MM in blocks with one joint. Two circles and one rectangle (thin lines) delimit three mathematical covers V_1, V_2 and V_3 to form the mathematical meshes. The physical meshes (thick lines) divide V_1 into two physical covers 1_1 and 1_2, V_2 into two physical covers 2_1 and 2_2, and V_3 into two physical covers 3_1 and 3_2. Eleven calculation elements are generated by the intersection of two sets of meshes and are denoted in this figure as 1_1, $1_1 2_2$, $1_1 2_2 3_1$, $1_2 2_1 3_2$, etc.

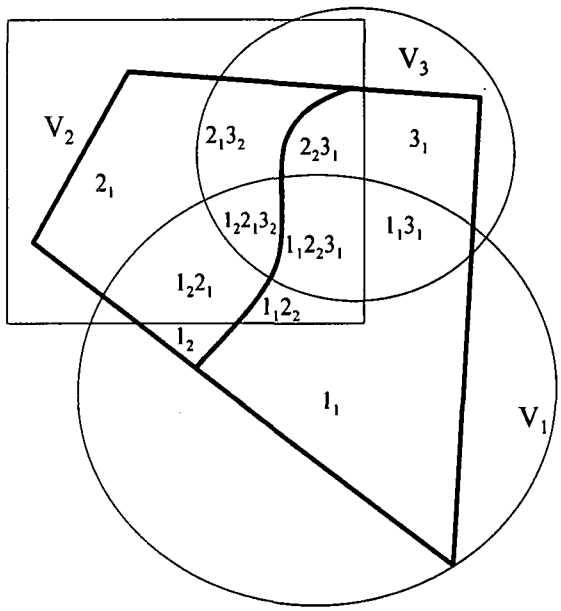

Fig.1 General covers with one joint[1)]

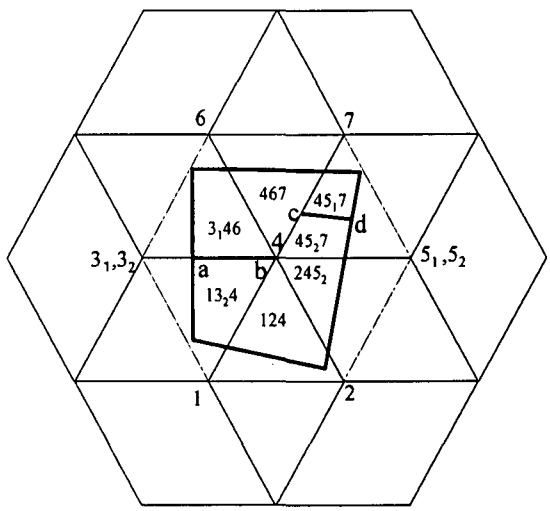

Fig.2 FEM type covers of MM in one block with two joints

Fig.2 gives an example of FEM type covers. Seven hexagonal mathematical covers around seven points 1-7 are given in this figure referring to thin lines. The physical meshes (thick lines, one block with two joints a-b and c-d) divide the mathematical cover around point 3 into two physical covers 3_1 and 3_2, divide the mathematical cover around point 5 into two physical covers 5_1 and 5_2. Nine physical covers ($1,2,3_1,3_2,4$, etc) and seven calculation elements (124, 245_2, $45_2 7$, etc) are generated.

2.2 Local Function and Global Function

If the local cover function $u_i(x,y)$ is defined on physical cover U_i :

$$u_i(x,y) \qquad (x,y) \in U_i$$

Then the global function $u(x,y)$ on the whole physical cover system can be defined from the local cover functions :

$$u(x,y) = \sum_{1}^{n} w_i(x,y) u_i(x,y)$$

where $w_i(x,y)$ is weight function defined as:

$$w_i(x,y) \geq 0 \quad (x,y) \in U_i$$
$$w_i(x,y) = 0 \quad (x,y) \notin U_i$$

$$with \quad \sum_{(x,y)\in U_i} w_i = 1$$

With the finite cover concept and the definition of local and global function, manifold method can model a wide variety of continuous and discontinuous materials, and FEM and DDA can be deemed as special cases of it.

2.3 Simultaneous Equilibrium Equations

For structural analysis problem, if the local displacement function on each physical cover is assumed to be constant, that is, the local displacement function on cover U_i is:

$$u_i(x,y) = D_i = \begin{Bmatrix} d_{i1} \\ d_{i2} \end{Bmatrix} = \begin{Bmatrix} u_i \\ v_i \end{Bmatrix}$$

then the simultaneous equilibrium equations of a problem with n physical covers take the form as:

$$\begin{bmatrix} K_{11} & K_{12} & K_{13} & \cdots & K_{1n} \\ K_{21} & K_{22} & K_{23} & \cdots & K_{2n} \\ K_{31} & K_{32} & K_{33} & \cdots & K_{3n} \\ \cdot & \cdot & \cdot & \cdot & \cdot \\ \cdot & \cdot & \cdot & \cdot & \cdot \\ \cdot & \cdot & \cdot & \cdot & \cdot \\ K_{n1} & K_{n2} & K_{n3} & \cdots & K_{nn} \end{bmatrix} \begin{bmatrix} D_1 \\ D_2 \\ D_3 \\ \cdot \\ \cdot \\ \cdot \\ D_n \end{bmatrix} = \begin{bmatrix} F_1 \\ F_2 \\ F_3 \\ \cdot \\ \cdot \\ \cdot \\ F_n \end{bmatrix} \qquad (1)$$

where K_{ij} is 2×2 sub-matrix. K_{ii} is defined by the shape and material properties of physical cover i, and K_{ij} $(i \neq j)$ depends on the overlapping or contact between cover i and cover j. F_i is the load matrix acted on cover i. Equation (1) was derived by Shi [1) 2)] according to minimum energy theory. Matrix *[K]* includes the stiffness of element, inertia matrix, stiffness of fixed points and contact stiffness. The load vector *[F]* includes initial load, point load, inertia load and contact load etc. The details of equation (1) can be found in Shi[1) 2)].

3. Modeling the Existing Joint

For an existing joint, there are two possibilities: 1) unfailed, namely the joint can be treated as continuous, and it can transfer both normal and shear stresses. 2) failed, that means the joint can only transfer normal compression stress or shear stress if the friction angle ϕ is not zero.

Modeling of the existing joint considers these two possibilities. **Fig.3** shows schematically the treatment of the joint by adding normal and shear springs at the joint. For the former case, if the thickness of joint layer is idealized as zero, there must be no relative normal displacement between two surfaces of the joint since they keep moving together under load. A very hard spring p (penalty) is therefore added in the normal direction to the joint to hold the possible relative normal displacement between two surfaces back to zero. In the tangent direction, however, a small relative shear displacement is usually permitted, especially when a soft layer is included in the joint. This condition is satisfied by adding a soft shear spring K_s in the tangent direction. For the later case in which joint failed, normal penalty and shear springs are added at the joint when the joint is loaded by compression and the shear stress is less than the friction between two surfaces. If the shear stress is larger than the friction, shear spring is removed and only normal spring is needed. If the joint opens, both normal and shear springs are removed from the joint.

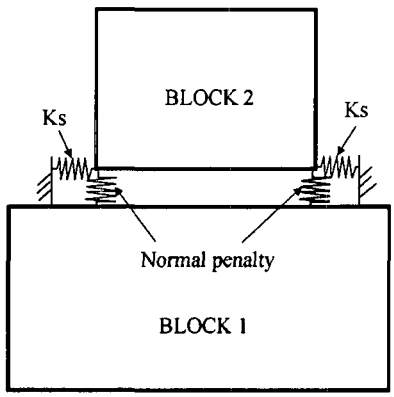

Fig.3 The normal and shear springs of contact blocks

In the present paper the failure process of existing joints is handled in the following way. Assume that failure of existing joints follows Mohr-Coulomb's law with three parameters. Taking σ'_y as the normal stress and τ'_{xy} as the shearing stress on a joint, the failure criterion is defined as bellow:

$$\begin{aligned} &\sigma'_y = T_0, && \textit{tensile failure} \\ &\left|\tau'_{xy}\right| = C, \ 0 < \sigma'_y < T_0 && \textit{shearing failure} \\ &\left|\tau'_{xy}\right| = C - \sigma' \tan\phi, \ \sigma'_y < 0, && \textit{shearing failure} \end{aligned} \quad (2)$$

where T_0represents the tension strength of joint, Crepresents cohesion, ϕ is the friction angle.

4. Crack Propagation in Solid Block

In rock foundation or concrete structure, cracks occur usually from weak zone like faults, joints and interfaces of different materials. With the propagation, the cracks break the mass material and lead to the final failure. Modeling the failure of foundation and structure must simulate both the opening of existing joints and the fracturing of mass materials.

Manifold Method is extended to simulate crack propagation in the present paper. When a new crack occurs or an old crack propagates the physical meshes and the mathematical meshes that contain this crack should be regenerated. If no physical cover is broken by the new crack, then only the physical meshes need to be reformed, the mathematical meshes keep unchanged. But if the new crack breaks a physical cover into two parts, then a new physical cover is produced, hence both the physical and mathematical meshes must be regenerated.

Fig. 4 is given here to illustrate the crack propagation and corresponding regeneration of the physical and mathematical mesh system in the numerical simulation. In Fig. 4(a) a new crack *ab* occurs. Since it does not break the physical cover that contains it into two parts, only physical meshes need to be regenerated by adding *ab* into the physical meshes. The mathematical meshes keep unchanged. Whereas in Fig.4(b), new occurred crack *bc* together with the existing crack *ab* break the cover that covers the area 4-5-8-10-9-6 into two parts, therefore a new cover must be added to the previous physical covers, and both the physical and mathematical meshes need to be regenerated.

In simulating the failure of solid block, formula (2) is also taken as the failure criterion. But in the present study, it is supposed that new cracks can only propagate along the mathematical meshes.

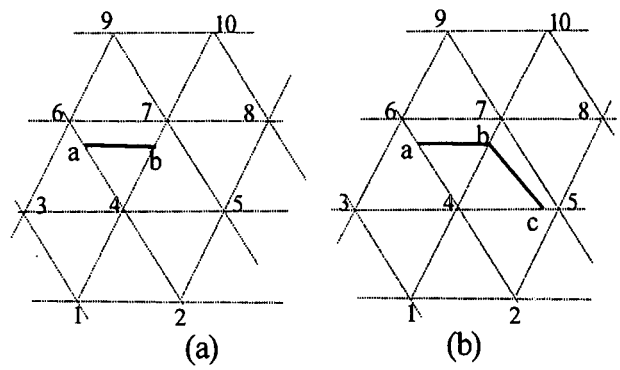

Fig.4 The relationship between new crack and covers

5. Application Examples

The safety of an arch dam depends mainly on the stability of the arch abutments. The stability and bearing capacity of the dam foundation are usually studied by experiment[9]. In this section the newly extended version of Manifold Method is applied to analyze the stability and bearing capacity of dam foundation and to simulate their failure process. The numerical results are compared with the experimental ones.

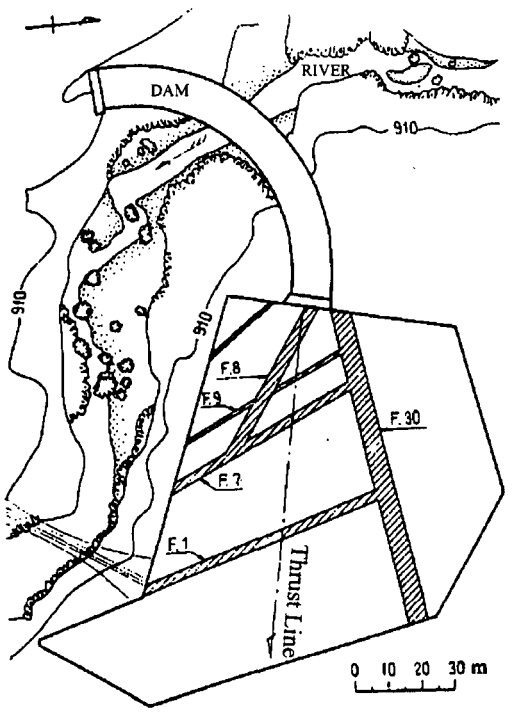

Fig.5 Model of an arch dam abutment[10)]

Table 1 Fault width and parameters

Fault	Width (m)	E (kg/cm^2)	T_0 (kg/cm^2)	C (kg/cm^2)	ϕ
F-30	5.0	3320	0.52	1.7	30
F-1	3.0	16530	2.87	9.0	30
F-7	2.0	22440	3.89	13.0	30
F-8	30	22440	3.89	13.0	30
F-9	0.5	16530	2.87	9.0	30
Good rock		68240	12.9	40.0	30
Concrete wall		267000	29.0	70.0	30

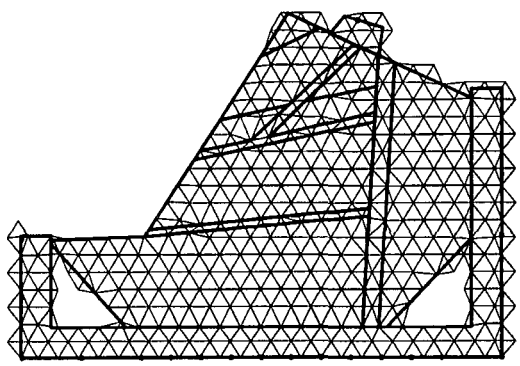

Fig.6 Mesh system used in MM simulation

5.1 Failure Simulation of an Arch Dam Abutment with Faults

Fig.5 shows the model of the abutment of an arch dam in Japan. The location of existing faults is denoted in this figure as F. 1, F. 7 etc. The stability and bearing capacity of this abutment before and after strengthened by concrete wall were studied by experiment in Public Works Research Institute Ministry of Construction, Japan [10)]. Here, by using the same model, the failure process and bearing capacity are simulated by Manifold Method.

The width of faults and the controlling parameters used in the calculation are listed in Table 1[10) 11)]. The strength of interface between two different material zones is taken as 80% of the lower one. The arch thrust force along the direction of arch axis was taken as P=5200 ton/m, calculated according to water pressure and temperature change. The mathematical and physical meshes used in MM simulation are shown in Fig.6, with thin lines referring to the mathematical meshes and thick lines referring to the physical meshes.

Three cases are calculated in the numerical simulation: (1) no foundation treatment, (2) foundation strengthened by 2m thick concrete wall, (3) foundation strengthened by 3.5m thick concrete wall.

Table 2 Bearing capacity in case 1 of experiment[10)]

Number	Bearing capacity (×P)	Number	Bearing capacity (×P)
1	0.5	6	1.1
2	0.6	7	1.0
3	0.6	8	1.15
4	0.7	9	1.20
5	0.9	10	1.20

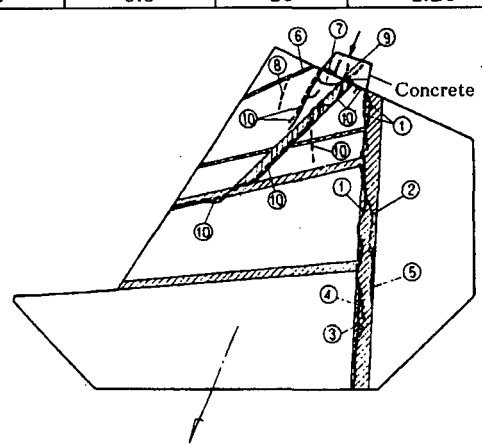

Fig.7 Experimental result of the abutment failure in case 1[10)]

Fig.7 shows the experimental result of failing process and bearing capacity of the abutment with no foundation treatment. Numbers in this figure denote the order of crack occurrence, and the corresponding bearing capacity is listed in Table 2.

Fig.8 shows the calculating result of the abutment failure in case 1. Cracks start occurring at the fault of F-30, as depicted in Fig.8(a) by thick line, because the material strength here is much smaller than that in the other areas. With the increase of load from 1.0P in Fig.8(b) to 1.3P in Fig.8(d), the abutment fails progressively at the fault location of F-7, F-8 and F-9. The computed failure process and the corresponding bearing capacity agree reasonably well with the experiment.

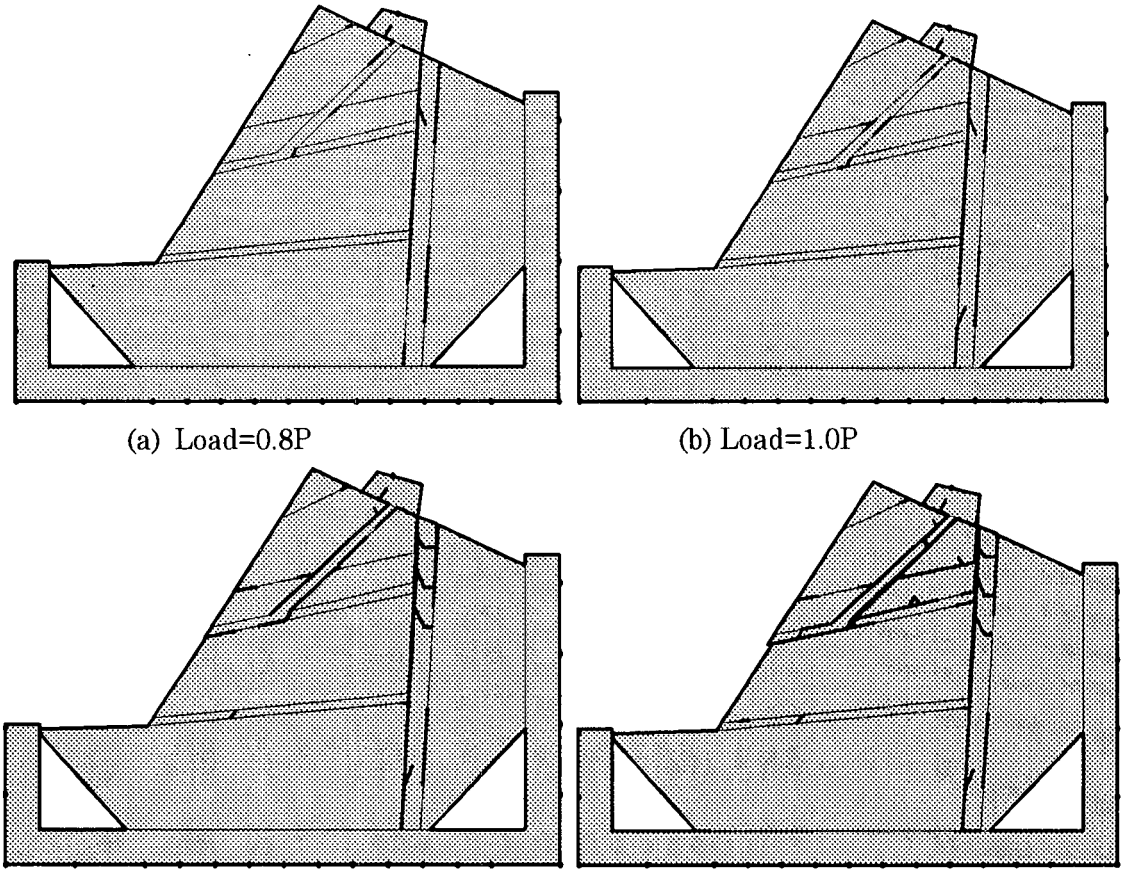

(a) Load=0.8P (b) Load=1.0P

(c) Load=1.2P (d) Load=1.3P

Fig.8 Computed failure process of abutment in case 1

Fig.9 gives the experimental result of the abutment failure process after strengthened by 2m thick concrete wall. Bearing capacity of the abutment obtained by experiment is listed in Table 3. From the results it can be seen that the bearing capacity of the foundation increases from 1.2P in case 1 to 2.8P after foundation treatment.

Table 3 Bearing capacity in case 2 of experiment[10)]

Number	Bearing capacity (×P)	Number	Bearing capacity (×P)
1~5	1.0	10	1.65
7	1.0	12~13	2.65
8	1.25	14~15	2.70
9	1.40	16	2.80

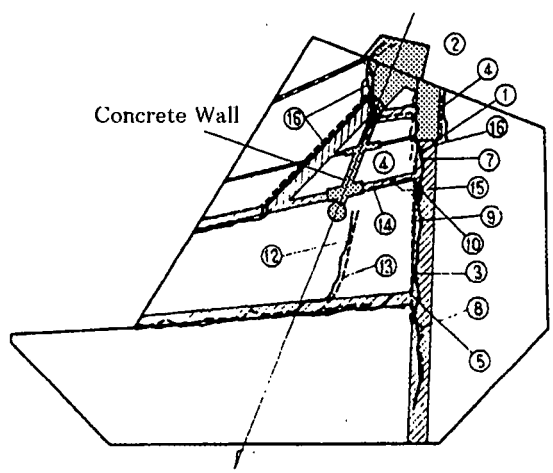

Fig.9 Experimental result of the abutment failure in case 2[10)]

Fig.10 shows the calculated result of failure process for case 2. In this case cracks start occurring at the fault F-30 when load reaches

0.6P, as shown in Fig.10(a). In Fig.10(b) when load reaches 2.0P, almost all the area of F-30 failes, and faults at F-8 and F-9 start opening. When load further increas to 2.6P, shown in Fig.10(c), the concrete wall begins to fail, leading to the failure of the foundation along F-30 to F-1. Following the failure of foundation, blocks lose their stability and begin to move. Fig.10(d) shows the movement of blocks after the foundation failure.

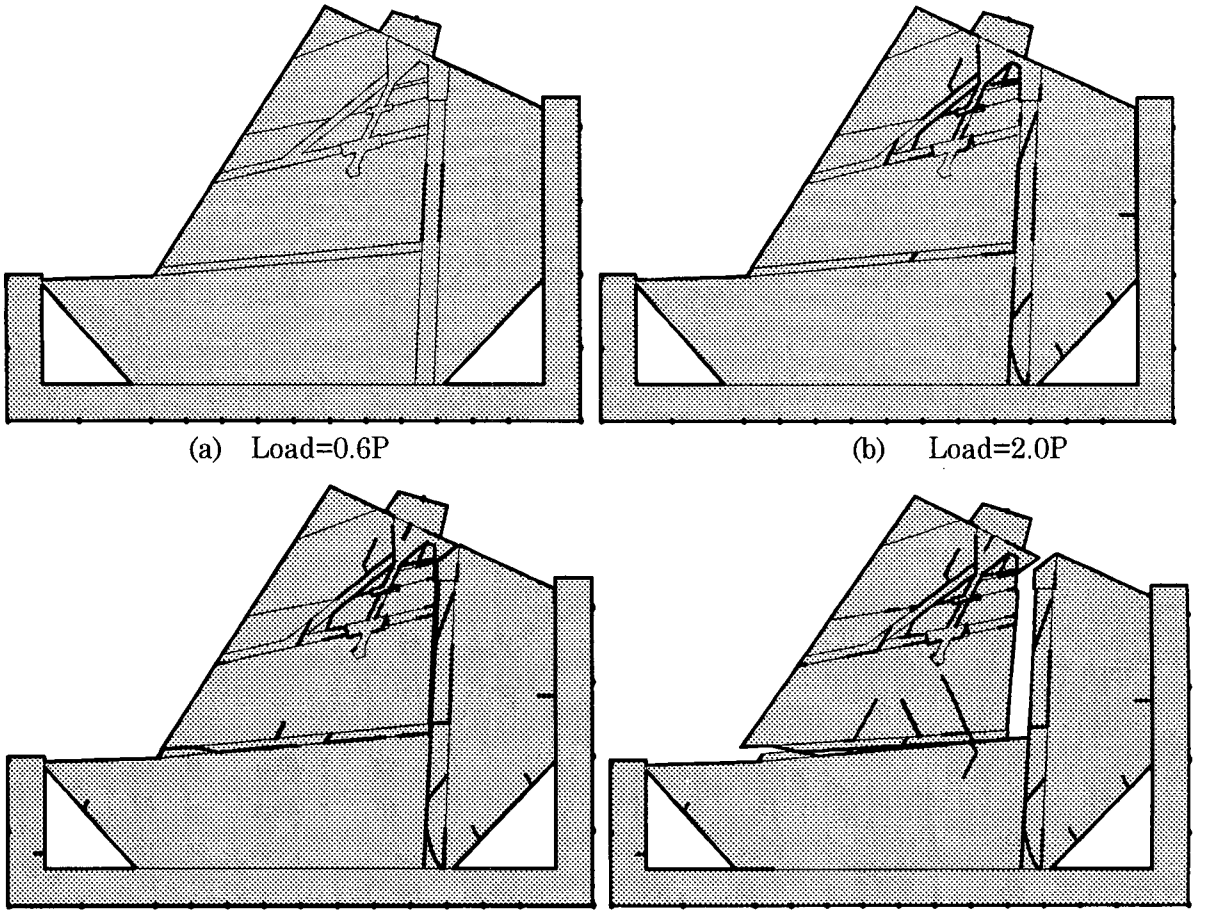

(a) Load=0.6P (b) Load=2.0P

(c) Load=2.6P (d) The Movement of Blocks

Fig.10 Computed failure process of the abutment in case 2

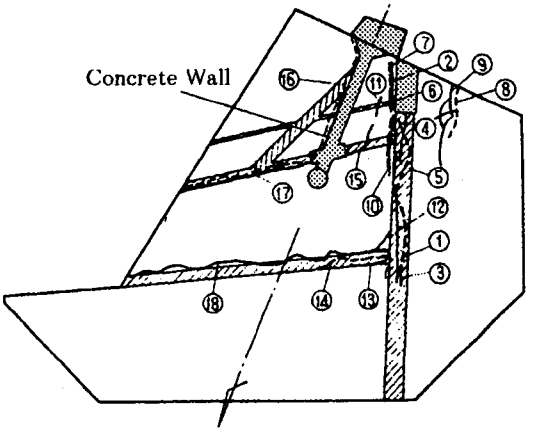

Fig.11 Experimental result after the foundation treatment by 3.5m concrete wall[10]

Experimental result of the abutment failure for case 3 is given in Fig.11 and the corresponding bearing capacity is listed in Table. 4. The bearing capacity increases to 4.0P due to the treatment of foundation by 3.5m thick concrete wall. The simulation result for the same case is shown in Fig.12. The prediction of bearing capacity is slightly larger than the experimental one. The failure process is similar to the experiment.

Table 4 Bearing capacity in case 3[10]

Number	Bearing capacity (×P)	Number	Bearing capacity (×P)
1	1.3	7~10	2.5
2	1.5	11	3.25
3	1.75	12~13	3.5
4~5	1.8~1.9	14	3.5~4.0
6	2.25	15~18	4.0

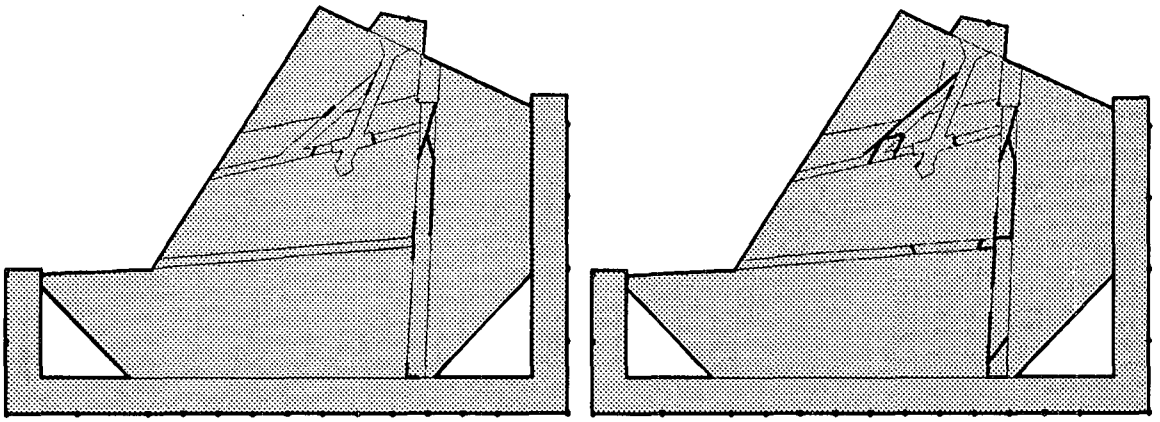

a) Load=1.2P b) Load=2.0P

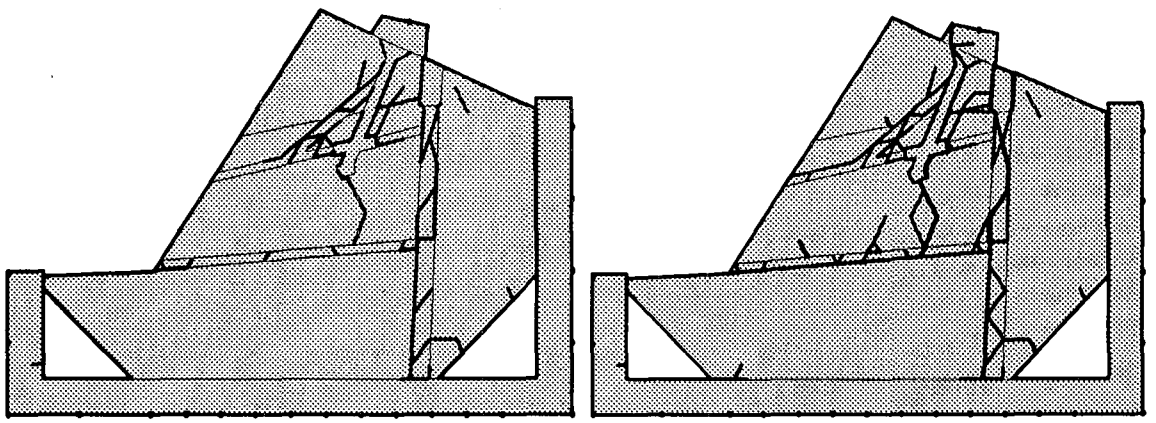

c) Load=3.0P d) Load=4.2P

Fig.12 The failure of abutment after strengthened by 3.5m concrete wall

5.2 Failure of a Dam Abutment with a Set of Joints

Second application of the extended MM is made in simulating the failure of an arch dam foundation with a set of joints. The experiment was carried out by Takano[11]. Fig.13 shows the diagram of the arch dam foundation. A set of joints exist paralleling to the direction of thrust force. Water pressure loads at the upper surface of the arch. The controlling parameters in the experiment are listed in Table. 5.

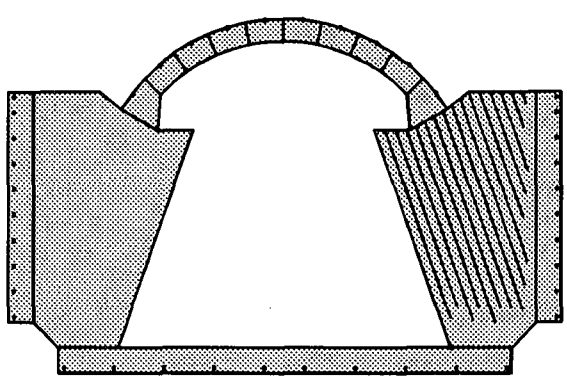

Fig.13 Abutment with one set of joints

Table 5 Calculation parameters

	E (kg/cm^2)	ν	Compression Strength (kg/cm^2)	T_0 (kg/cm^2)	C (kg/cm^2)	ϕ
Arch	200000	0.2	250	------	------	------
Left Abutment	20000	0.2	60	6	20	30
Right Abutment	20000	0.2	30	3	10	30
Joint	------	------	------	0.6	1.2	18

The experimental result showed that the abutment failed as shown in Fig.14 when the water pressure q=9.3kg/cm^2 [11].

Fig.15 gives the simulating result by MM. Because the strength of joint is less than that of the mass material, some joints firstly open because of the tension and shear failure (See Fig.15 a)). The load conducted by arch is mainly supported by the blocks contacting with the arch, and the principal stress is parallel to the thrust direction (Fig.15 a)). This is the same with the experimental conclusion. When the pressure on arch increases to 7.0 kg/cm^2, some cracks occur in mass blocks (Fig.15b)), and when the load reaches to 7.5 kg/cm^2, the foundation fails (Fig.15 c) d)). The bearing capacity obtained by MM is less than the experimental result and the failure pattern has some differences. In the experiment, the failure is caused by compression but in MM analysis, the failure of the foundation is mainly caused by shear failure.

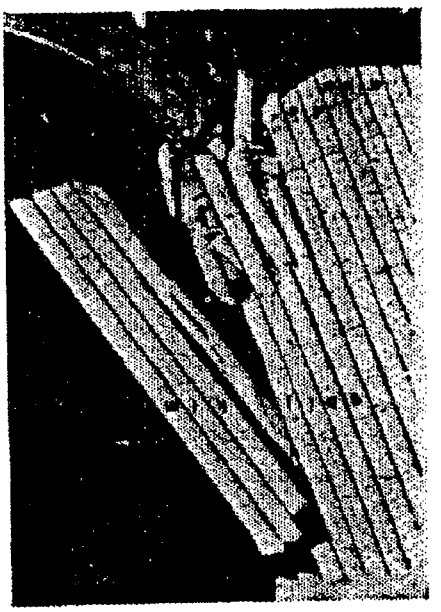

Fig.14 Experimental result[11]

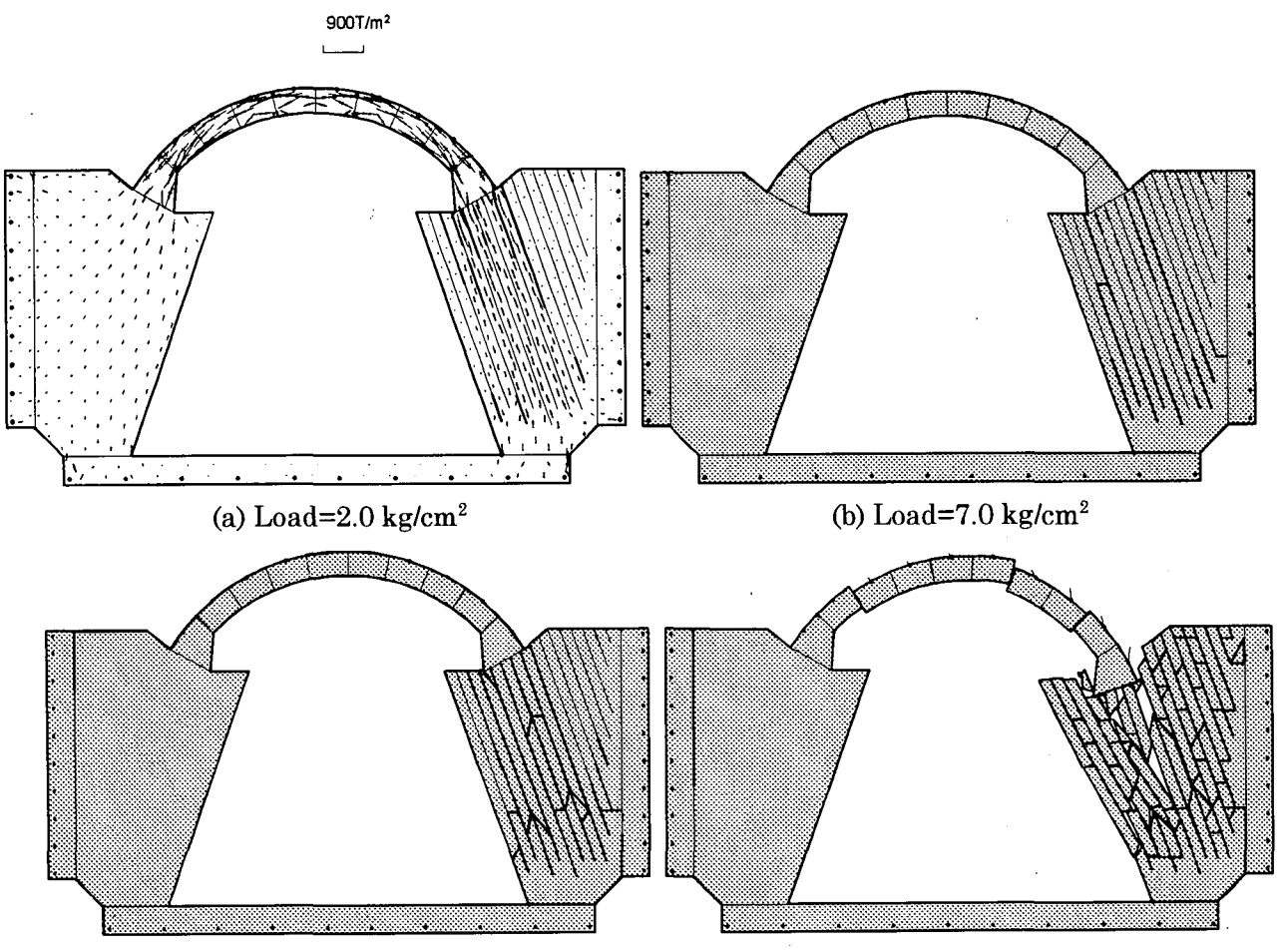

(a) Load=2.0 kg/cm^2

(b) Load=7.0 kg/cm^2

(c) Load=7.5 kg/cm^2

(d) Failure of arch and dam

Fig.15 Computed failure of arch foundation by MM

6. Conclusion

Manifold Method is a newly developed numerical tool in analyzing continuous and discontinuous problems. In the present paper the original MM was extended by adding the consideration of crack propagation in failure process into the numerical procedure. The extended version of MM is capable of dealing with the failure of structure or foundation with joints or faults. Application examples were given in simulating the failure process of a dam abutment with faults and a dam foundation with joints. The prediction results of the bearing capacity and the failure process are in good agreement with the experiments. It is convinced that the extended version of MM can reproduce the initiation of cracks, the failure process and block movement reasonably well. From engineering practical point of view, the numerical method developed in the present study would be a very useful tool in simulating the failure process of structure with discontinuities.

Acknowledgments

The author would like to thank Dr. G. H. Shi and Professor Yuzo OHNISHI for suggestions.

Reference

1) Shi, G. H., Manifold Method of Material Analysis. *Proc. Ninth Army Conference on Applied Mathematics and Computing,* Minneapolis, Minnesota, U.S.A., pp. 51-76, June 18-21,1991.
2) Shi Genhua, Manifold Method, *Discontinuous Deformation Analysis (DDA) and Simulations of Discontinuous Media,* pp. 52-204, TSI Press 1996.
3) Jeen-Shang Lin, Continuous and Discontinuous Analysis Using the Manifold Method. *Working Forum on the Manifold Method of Material Analysis.* Jenner, California, USA,(1996). Vol. 1, pp. 1-20.
4) Chiao-Tung Chang, Nonlinear Level Manifold Method, *Working Forum on the Manifold Method of Material Analysis.* Jenner, California, USA,(1996). Vol. 1, pp. 127-146.
5) Mary MacLaughlin, Manifold Application: Tunnel Roof Deflection. *Working Forum on the Manifold Method of Material Analysis.* Jenner, California, USA,(1996). Vol. 1, pp. 241-244.
6) Guo-Xin Zhang, Yasuhito Sugiura and Hiroo Hasegawa, Crack propagation and thermal fracture analysis by Manifold Method, *Proceedings of the Second International Conference on Analysis of Discontinuous Deformation,* July 10-12,1997,Kyoto Japan, pp.282-297.
7) Yaw-Jeng Chiou, Crack Propagation Using Manifold Method. *Proceedings of the Second International Conference on Analysis of Discontinuous Deformation,* July 10-12,1997,Kyoto Japan, pp.298-308.
8) Guang-Qi Chen, Yozo Ohnishi and Takahiro Ito. Development of High Order Manifold Method. *Proceedings of the Second International Conference on Analysis of Discontinuous Deformation,* July 10-12,1997,Kyoto Japan. pp.132-154.
9) R. Iida, *Design Method of Concrete Dam,* GIHODO Press, February 1992.
10) K. Nakamura, R. Iida and T. Tsutaya, Model Study on Foundation Rocks of Kawamata Dam, Report of The Public Works Research Institute Ministry of Construction, Vol. 120, No.78, pp. 1-11, October 1964.
11) Minoru Takano, Studies on Experimental Method of Measuring Safety of Arch Dam Foundation, *Transactions of the Japan Society of Civil Engineers,* No. 78, pp. 43-69, January 1962.

(Received April 24, 1998)